Discovery of Electric Pulsation in a Toroidal Helical Plasma

A. Fujisawa,[1] H. Iguchi,[1] H. Idei,[1] S. Kubo,[1] K. Matsuoka,[1] S. Okamura,[1] K. Tanaka,[1] T. Minami,[1] S. Ohdachi,[1] S. Morita,[1] H. Zushi,[2] S. Lee,[1] M. Osakabe,[1] R. Akiyama,[1] Y. Yoshimura,[1] K. Toi,[1] H. Sanuki,[1] K. Itoh,[1] A. Shimizu,[1] S. Takagi,[3] A. Ejiri,[1] C. Takahashi,[1] M. Kojima,[1] S. Hidekuma,[1] K. Ida,[1] S. Nishimura,[1] M. Isobe,[1] N. Inoue,[1] R. Sakamoto,[1] S.-I. Itoh,[2] Y. Hamada,[1] and M. Fujiwara[1]

[1]*National Institute for Fusion Science, Oroshi-cho, Toki-shi, 509-5292 Japan*

[2]*RIAM, Kyushu University, Kasuga 816 Japan*

[3]*Department of Energy Engineering Science, Nagoya University, Nagoya 464-01, Japan*

(Received 12 November 1997; revised manuscript received 28 April 1998)

A pulsating behavior of the electrostatic potential has been discovered in a low-density, high-electron-temperature plasma of the CHS heliotron/torsatron. The potential profiles were observed to swing repeatedly between two distinctive states in a constant external magnetic field under a continuous supply of particles and energy. The change of the potential profile, which occurs on a much faster time scale (microseconds) than the diffusive time scale (milliseconds), is accompanied by changes in density and temperature. This discovery clearly demonstrates that even in a low beta regime a toroidal helical plasma can produce a self-sustaining dynamic steady state, like the sawtooth oscillation in tokamaks. [S0031-9007(98)07099-9]

PACS numbers: 52.55.Hc, 52.25.Fi, 52.35.Nx

Among fusion oriented devices, toroidal helical plasmas (e.g., stellarator, torsatron, and heliotron) are supposed to realize a "plasma with static state." This is because static external coils alone can produce the necessary magnetic field for confinement, without an internal plasma current which sometimes leads to violent instabilities such as disruptions [1]. The current driven instability relaxes the plasma to a lower magnetic energy state and forms dynamic steady states with the well-known sawtooth oscillations, which were discovered in the ST tokamak [2].

The edge localized mode (ELM) is another example of a dynamic steady state [3]. The ELM is considered to be deeply associated with the H-mode transition [4–7], where the radial electric field plays an important role. For toroidal helical plasmas, the radial electric field has a primary importance since it affects the bipolar collisional transport caused by their own helical ripples. Nonlinear dependence of these bipolar fluxes on E_r allows the existence of multiple equilibrium states and has been expected to give birth to a dynamic behavior associated with transitions between these states in the toroidal helical plasmas [8,9].

We have recently discovered a "dynamic steady state" in the toroidal helical plasma, which is termed here "electric pulsation." In this state, the plasma is thought to exhibit successive transitions between two distinctive profiles. This Letter is the first report of a new kind of oscillatory state accompanied by global structural reformation in the toroidal helical plasma.

The compact helical system (CHS) is a heliotron/torsatron device whose major and averaged minor radii are 1.0 and 0.2 m, respectively [10]. The CHS has a theoretical β limit of more than 5% and has achieved the highest β of 2.1% in toroidal helical plasmas [11]. The electrostatic potential of the plasma interior has been directly measured with a heavy ion beam probe (HIBP) [12,13]. The temporal resolution of our HIBP is up to 300 kHz in the presented experiments. Simultaneously, the HIBP signal gives some information about density profiles $n_e(r)$ and internal magnetic field fluctuation.

The detected beam intensity I_D is expressed as $I_D(r) \propto Q_{12}(r) \exp[-\alpha_1(r) - \alpha_2(r)]\Delta v$, where $Q_{12}(r)$ is the local rate of beam ionization from singly to doubly charged states, and $\alpha(r)$ and Δv are the beam attenuation and the sample volume, respectively. The attenuation factor is defined as $\alpha_i(r) \equiv \int_r Q_i \, dl_i$, where $Q_i (i = 1, 2)$ is the total ionization cross section from the ith charged states to a more highly charged state. The ionization rate is proportional to electron density [e.g., $Q_{12}(r) \propto n_e(r)$] provided that the electron temperature is sufficiently high ($\sim$100 eV). The beam movement on the detector is associated with a change of the internal magnetic field; thus HIBPs can detect internal magnetic fluctuations [14].

The electric pulsation has been observed in hydrogen or deuterium plasmas using electron cyclotron heating (ECH) after adequate wall conditioning. The density is rather low ($n_e = 3 \sim 7 \times 10^{12}$ cm^{-3}) and electron temperature is high ($\sim$1 keV) for the case of an on-axis field strength of 0.88 T. This dynamic steady state usually can be attained by applying ECH at the second harmonic resonance (53.2 GHz, $\sim$300 kW) on target plasmas sustained by neutral-beam injection (NBI) (with a port-through power of $\sim$700 kW). The NBI deposition in this plasma is $\sim$10%–30% of the port-through power.

Figure 1 shows an example of an electric pulsation observed in the potential at the center of a hydrogen plasma, together with the time evolution of the line-averaged electron density. After the ECH is on, the electron density

 0031-9007/98/81(11)/2256(4)$15.00

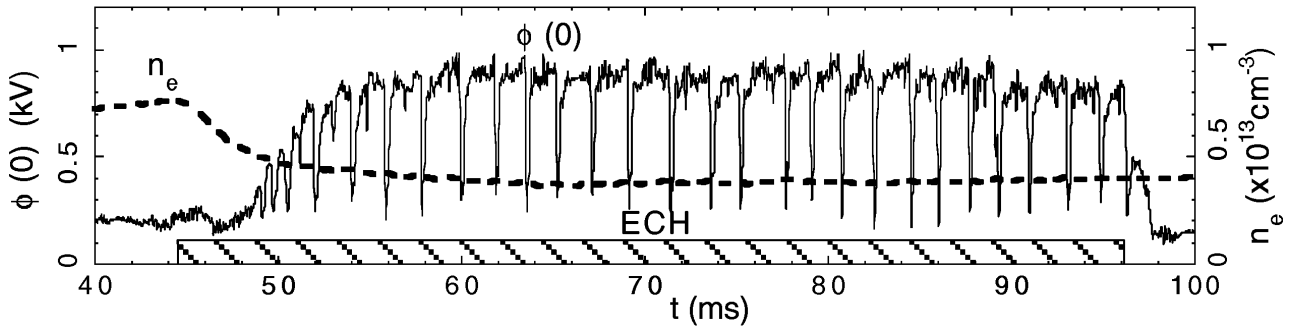

FIG. 1. Pulsating behavior of the central potential of CHS plasmas (solid line). This phenomenon, referred to as electric pulsation, is observed in a combined ECH + NBI heating phase. The dashed line represents the line-averaged electron density measured with a hydrogen cyanide interferometer.

decreases and relaxes to a steady state of $n_e \simeq 4 \times 10^{12}$ cm^{-3} in approximately 5 ms. The net toroidal current including the beam driven and the bootstrap contributions is less than 0.5 kA. This current may cause a slight change in the safety factor of $\delta q(r)/q \sim 0.2\%$. The internal energy measured by a diamagnetic loop and the average β are about 400 J and 0.2%, respectively.

In the steady state ($55 < t < 95$ ms), negative pulses of potential of -0.6 kV occur quasiperiodically approximately every 2 ms. The time scale of a pulse (approximately a few dozen microseconds) is much faster than the diffusive one (approximately a few milliseconds). Potentials at other locations also exhibit quasiperiodic pulses at similar intervals but with different amplitudes and polarities. In contrast to the pulses near the plasma center, positive pulses are observed in the outer plasma radii. The pivot point at which the pulse changes its polarity is located around the normalized plasma radius $\rho = 0.53$, as is shown in Figs. 2a–2c. In Fig. 2d, the averages of local maxima and minima in the periods including a pulse are plotted as a function of the normalized radius. Hence the fitting curves represent two states before and after the crashes. The plotted data were sequentially taken shot by shot with an identical operational condition. Around the center, the derivative of the potential (the electric field) does not change considerably before and after the crashes. A large change of the electric field, as a result, occurs around the pivot during a crash.

Figure 3 shows that other plasma parameters are also pulsating with the potential. The soft x-ray emission along the central line of sight ($\rho^+ = 0$) decreases with the potential crashes, while the soft x ray on an outer line of sight ($\rho^+ = 0.4$) increases. Here ρ^+ indicates the normalized smallest tangency radius of chordal measurements. This may be interpreted as a heat flux propagating from the inner to the outer region. An increase in the electron cyclotron emission (ECE) (93.5 GHz) signal from an outer region of the plasma ($\rho > 0.5$) supports this interpretation, although a plasma at such a low density is not sufficiently optically thick for the ECE to reflect the electron

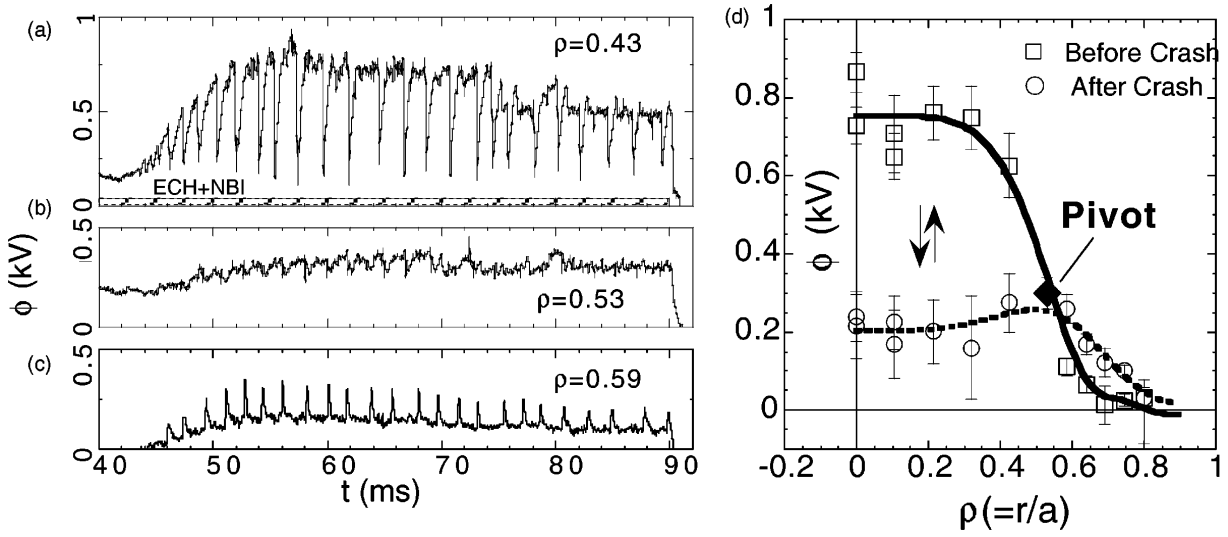

FIG. 2. Spatial structure of a global electric pulsation. (a) Time evolution of potential at $\rho = 0.43$; (b) at $\rho = 0.53$; (c) at $\rho = 0.63$; and (d) spatial structural change of the potential before and after crashes. Here ρ is the normalized minor radius.

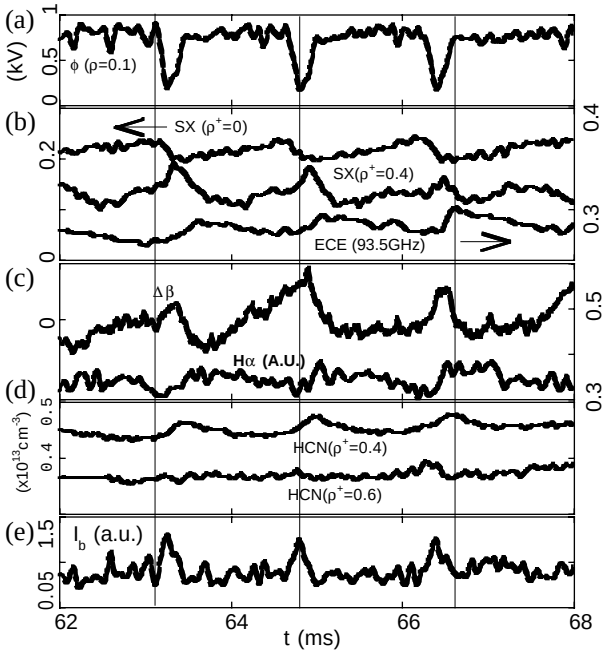

FIG. 3. Correlation of the potential change with other plasma parameters. (a) Potential signal at $\rho = 0.1$. (b) Chord integrated soft x-ray emissions of two lines of sight of $\rho^+ = 0.4$ and $\rho^+ = 0.0$, together with ECE from the plasma edge region ($\rho > 0.5$). Here ρ^+ indicates the normalized distance of a chord from the plasma center. (c) Change of $\Delta\beta$ estimated from plasma shift. The plasma shift is measured by Mirnov coils located at the inner and outer points on the equatorial plane and H_α emission from the plasma edge. (d) Line-averaged electron densities with $\rho^+ = 0.4$ and $\rho^+ = 0.6$. (e) Detected beam intensity of the HIBP.

temperature. In the CHS magnetic configuration, the ECE emission has several resonant points; therefore, the change of the temperature profile cannot be deduced.

Mirnov coils at the inner and outer points of the equatorial plane indicate that the plasma starts moving inward when the potential reaches its minimum during a pulse. The inward shift implies that the plasma loses an internal energy of about 20 J (approximately $\Delta\beta \simeq 0.01\%$) with a potential pulse. Good correlation of H_α emission with the potential pulses also shows that the electric pulsation should affect the plasma periphery. Thus this oscillation limits or deteriorates the confinement property of the plasma.

The line-averaged density signals on chords of $\rho^+ < 0.4$ show an increase synchronized with a potential crash, while the other ones on outer chords show no clear correlation; the line-averaged density of $\rho^+ = 0.6$ is given as an example in Fig. 3d. The detected beam intensity, which has faster temporal resolution than the interferometer, also exhibits a good correlation with the potential signal; the intensity increases (or decreases) in a similar time scale with the potential drops (or rises) at observation points of $\rho < 0.4$ (or >0.4). Using Lotz's empirical formula [15], the condition of $\alpha < 1$ is satisfied in this low-density plasma for both completely flat and parabolic density profiles. Consequently, the change of the detected beam intensity $\delta I_b(r)$ reflects a mainly local density change, except at the plasma edge [13,16].

This fact suggests that the density profile is also reformed with the electric field (e.g., $I_D \propto n_e$). Figure 4 demonstrates the change of detected beam intensity before and after crashes. The dashed line indicates the density profile of higher potential states after the Abel inversion of the interferometer signals obtained shot by shot. By taking account of the change of the beam intensity, it is inferred, thus, that a slightly hollow profile becomes peaked after crash, with a change of central density from $n_e \simeq 4$ to 6×10^{12} cm^{-3}.

The presented example of the electric pulsation was obtained in plasmas with the line-averaged density of $n_e \simeq 4 \times 10^{12}$ cm^{-3}. So far we have a dependence of pulsation characteristics on electron density, as is shown in Fig. 5. The oscillation period becomes shorter (Fig. 5a) and its amplitude becomes smaller (Fig. 5b) as the density increases for a fixed heating power; simultaneously the pulsating region becomes narrower and is confined to a region around the center. The effect of this "localized" electric pulsation to the plasma periphery is small, judging from the fact that the correlation of H_α becomes ambiguous. Finally, the pulsation disappears above a certain critical density; that is, $n_e \sim 8 \times 10^{12}$ cm^{-3} in this case with an ECH power of 300 kW. In another series of experiments with an ECH power of 200 kW, the pulsation cannot be seen above $n_e \sim 5 \times 10^{12}$ cm^{-3}. In experiments to date, the threshold power used to obtain the electric pulsation appears to become higher as the density increases.

The mechanism of the pulsation should not be ascribed to the magnetohydrodynamics (MHD) activity. Actually, no special activity has ever been detected in any Mirnov coils for poloidal field before or during the potential crashes. No precursor oscillation has been found in soft

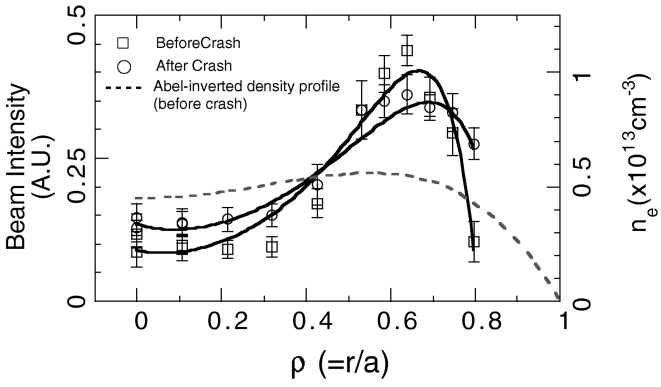

FIG. 4. Profiles of the detected beam intensity after and before crashes. The dotted line indicates the density profile with Abel inversion in the higher potential states. This suggests that the density profile after a crash becomes a centrally peaked one.

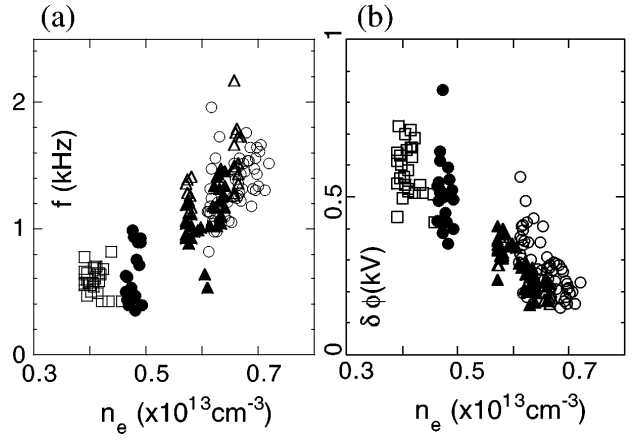

FIG. 5. Dependence of pulsation characteristics on electron density. (a) Frequency of pulsation observed in $\phi(0)$ versus line-averaged density. (b) Pulse amplitude of central potential versus line-averaged density. Here the port-through NBI and ECH powers are 700 and 300 kW, respectively.

x-ray signals. The HIBP beam movement has shown no correlation with the pulsation. The magnetic field fluctuation indicates a turbulent nature with its level of $10^{-5} \sim 10^{-4}$ ($f > 1$ kHz). A fast Fourier transform analysis shows that any significant coherence does not exist between a Mirnov signal and the potential; their coherence is ~ 0.1.

In another electric pulsation near the power threshold in a deuterium plasma, the period of a lower potential state (~ 1 ms) was nearly the same as that of the higher one. The feature of a pulse is very similar to a transition previously observed in a CHS plasma [17]. As the ECH power increased, the period of the higher state became longer. The time scales of the downward and upward changes are a few dozen and a hundred microseconds, respectively [18]. The properties simply demonstrate that electric pulsation should be recognized as repetitive transitions between two distinctive states.

The most probable candidate for the mechanism of pulsation is the bifurcation property of E_r in a toroidal helical plasma. A neoclassical calculation is able to show such a characteristic curve indicating a bifurcation of E_r within a plausible plasma parameter range for CHS. The transition characteristic was compared in more detail with the neoclassical estimation in a previous Letter [17].

Various repetitive oscillations have been observed in toroidal plasmas: sawtooth oscillations and ELMs (e.g., type I, type III, and dithering) [3] and relaxation oscillations in the velocity space of runaway discharges of tokamaks [19]. The pulsation caused by velocity space instabilities consists of two phases of slow growth and rapid drop, that is, buildup of anisotropy and its relaxation. The sawtooth oscillation and type-I and type-III ELMs have been discussed as being associated with current driven, ballooning, and resistive MHD instabilities, respectively. The type-III and type-I ELMs are characterized by precursors and the increase of highly turbulent magnetic fluctuations, respectively. The presented phenomenon is somewhat analogous to the dithering ELMs as a successive transition between L- and H-modes [20]. The radial extent of the pulsation, however, varies according to the plasma density, while the ELM is characterized by a local structural change around a fixed edge transport barrier.

In conclusion, we have discovered a dynamic steady state in a toroidal helical plasma. Accordingly, near-currentless toroidal helical plasmas are not static but can be dynamic, even in a low-β regime. In a future laboratory plasma relevant to a fusion reactor, power from fusion reactors could be a source of energy to drive the "global" electric pulsation; then its effect on walls, diverters, and so on could be as severe as anticipated.

The authors are very grateful to Professor A. Iiyoshi for his continuous support and encouragement. A. F. is specially grateful to Dr. B. J. Peterson for valuable comments.

[1] L. A. Artsimovich, Nucl. Fusion **12**, 215 (1972).
[2] S. Von Goeler, S. W. Stodiek, and N. Sautoff, Phys. Rev. Lett. **33**, 1201 (1974).
[3] H. Zohm, Plasma Phys. Controlled Fusion **38**, 105 (1996).
[4] F. Wagner *et al.*, Phys. Rev. Lett. **49**, 1408 (1982).
[5] For review see K. Itoh and S.-I. Itoh, Phys. Controlled Fusion **38**, 1 (1996).
[6] S.-I. Itoh and K. Itoh, Phys. Rev. Lett. **60**, 2276 (1988).
[7] K. C. Shaing and E. Crume, Jr., Phys. Rev. Lett. **63**, 2369 (1989).
[8] D. E. Hastings, W. A. Houlberg, and K. C. Shaing, Nucl. Fusion **25**, 445 (1985).
[9] L. M. Kovrizhnykh, Nucl. Fusion **24**, 435 (1984).
[10] K. Matsuoka *et al.*, in *Proceedings of the Twelfth International Conference on Plasma Physics and Controlled Nuclear Fusion Research, Nice, 1988* (International Atomic Energy Agency, Vienna, 1989), Vol. 2, p. 411.
[11] S. Okamura *et al.*, Nucl. Fusion **35**, 283 (1995).
[12] A. Fujisawa *et al.*, Phys. Plasmas **4**, 1357 (1997).
[13] A. Fujisawa, H. Iguchi, S. Lee, and Y. Hamada, Rev. Sci. Instrum. **68**, 3393 (1997).
[14] V. J. Simcic *et al.*, Phys. Fluids B **5**, 1576 (1993).
[15] W. Lotz, Astrophys. J. Suppl. **14**, 207 (1967).
[16] Around the edge the electron temperature change should be taken into account in estimation of the attenuation term since the cross section Q is strongly dependent on the electron temperature when it is below a few hundred eV.
[17] A. Fujisawa *et al.*, Phys. Rev. Lett. **79**, 1054 (1997).
[18] By fitting a function form of $\tanh(t/\tau)$ to the slopes, the time scales τ are estimated at 60 and 150 μs for forward (a higher potential state to a lower one) and backward transitions, respectively.
[19] V. V. Parail and O. P. Pogutse, Sov. J. Plasma Phys. **2**, 125 (1976).
[20] S.-I. Itoh *et al.*, Phys. Rev. Lett. **67**, 2485 (1991).